IOP Publishing Journal of Neural Engineering
J. Neural Eng. 12 (2015) 046029 (10pp) doi:10.1088/1741-2560/12/4/046029

Predicting workload profiles of brain–robot interface and electromygraphic neurofeedback with cortical resting-state networks: personal trait or task-specific challenge?

Meike Fels[1], Robert Bauer[1] and Alireza Gharabaghi

Division of Functional and Restorative Neurosurgery & Division of Translational Neurosurgery, Department of Neurosurgery, and Neuroprosthetics Research Group, Werner Reichardt Centre for Integrative Neuroscience, Eberhard Karls University Tuebingen, Germany

E-mail: alireza.gharabaghi@uni-tuebingen.de

Received 20 January 2015, revised 28 May 2015
Accepted for publication 12 June 2015
Published 14 July 2015

Abstract

Objective. Novel rehabilitation strategies apply robot-assisted exercises and neurofeedback tasks to facilitate intensive motor training. We aimed to disentangle task-specific and subject-related contributions to the perceived workload of these interventions and the related cortical activation patterns. *Approach*. We assessed the perceived workload with the NASA Task Load Index in twenty-one subjects who were exposed to two different feedback tasks in a cross-over design: (i) brain–robot interface (BRI) with haptic/proprioceptive feedback of sensorimotor oscillations related to motor imagery, and (ii) control of neuromuscular activity with feedback of the electromyography (EMG) of the same hand. We also used electroencephalography to examine the cortical activation patterns beforehand in resting state and during the training session of each task. *Main results*. The workload profile of BRI feedback differed from EMG feedback and was particularly characterized by the experience of frustration. The frustration level was highly correlated across tasks, suggesting subject-related relevance of this workload component. Those subjects who were specifically challenged by the respective tasks could be detected by an interhemispheric alpha-band network in resting state *before* the training and by their sensorimotor theta-band activation pattern *during* the exercise. *Significance*. Neurophysiological profiles in resting state and during the exercise may provide task-independent workload markers for monitoring and matching participants' ability and task difficulty of neurofeedback interventions.

Keywords: brain–robot interface, brain–machine interface, brain–computer interface, resting state network, work load, neurorehabilitation, neurofeedback

(Some figures may appear in colour only in the online journal)

Background

Functional restoration in patients with severe and persistent motor deficits, e.g. after a stroke, is very limited, despite rehabilitation training in accordance with evidence-based guidelines [1]. Current therapeutic strategies include neurofeedback training [2, 3], e.g. feedback of neuromuscular activity in the affected upper extremity on the basis of electromyography (EMG) [4–6] or feedback of motor imagery-related sensorimotor oscillations (SMR) of the ipsilesional

[1] These authors contributed equally to this work.

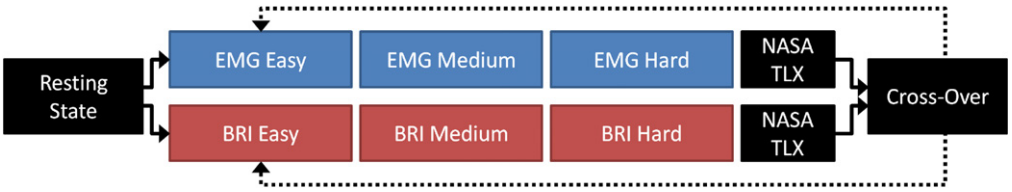

Figure 1. Experimental design with the general flow of the task.

cortical electroencephalogram by providing haptic/proprioceptive feedback with a brain–robot interface (BRI) [7–9]. The goal of these restorative approaches is the modification of neuronal activity via operant conditioning, e.g. challenging the patient to attain specific states that might facilitate motor recovery.

Restorative interventions differ from classical *assistive* approaches which aim to replace lost function by external devices. While *assistive* brain-interfaces select and weight cortical activity features on the basis of their ability to maximally contrast different brain states, the feature space for *restorative* approaches is usually deliberately constrained due to physiological considerations [10, 11] so as to facilitate reinforcement and learning of these specific brain states [12, 13]. Therefore, while calibration according to individual brain patterns or the classical adaptive fitting approach of assistive brain-interfaces [14, 15] may indeed result in maximum separation between classes, it may not match with the goal of reinforcement training of physiologically defined features such as sensorimotor beta-band activity. However, without these standard optimization strategies, restorative BRIs achieve typically low classification accuracies [12]. This may cause increased cognitive load [12, 16, 17], reflected by a restricted ability to concentrate on the task [18]. We were therefore interested in how the workload profile of such a restorative BRI compares to a neurofeedback task based on EMG-feedback.

Stroke-related impairments of cognitive abilities may, however, influence the physiology of neurofeedback to such an extent that it interferes with our understanding of underlying basic mechanisms [19, 20]. We therefore decided to begin by studying the workload profiles of different neurofeedback interventions and the related neurophysiological markers in healthy subjects. To ensure that subjects remained challenged and focused on the aspect of motor learning and adaptation, we conducted the study on right-handed subjects who performed the tasks with their non-dominant, i.e. left, hand.

Several workload measurements were introduced to the brain–computer/machine interface field to complement the classical evaluation of classifier performance [21, 22]. Such an assessment of efficiency, i.e. the subjective workload profile, might, for example, be quantified by means of the NASA task load index (NASA-TLX) [23, 24], providing high validity and easy implementation [25]. Since earlier brain interface-based studies reported that a subset of subjects may have difficulty with the task or even suffer from task-illiteracy [26], we performed clustering analysis to detect users who might be particularly challenged by this task.

The performance in the very same EMG and BRI tasks was recently shown to be predictable on the basis of specific alpha-band network topographies during resting-state electroencephalography (EEG) before the tasks [27]. These findings inspired us to use a combination of the NASA-TLX and resting state EEG measurements as a potential screening tool for future treatment matching. We therefore examined the link between workload cluster membership and resting state networks. Furthermore, on account of its robustness against noise [28], we used the phase slope index (Ψ) [29] as a cortical connectivity measure. Since Ψ is based on the slope of phase change with increasing frequency, it provides a signed measure and has a zero mean expectancy if there is no systematic time lag between two channels [30]. Ψ therefore provides a direct measure of connectivity that is immune to volume conduction effects, thus providing straightforward statistical properties.

Since different physiological features have been researched for online estimation of workload [31–33], we also examined cortical neurophysiology *during* the tasks in relation to cluster membership, albeit we did not primarily intend to research the physiological online correlates of task load in this study. Connectivity measures require larger time windows, and are therefore less suitable for online classification. We therefore restricted our task-related neurophysiology analysis to the power domain. By this means, we hoped to disentangle subject-related and task-specific components to gain information for future online-monitoring studies.

Methods

Study design and subjects

We recruited twenty-two right-handed healthy subjects (13 female), aged between 20 and 58 (mean age = 28.52; SD = 10.25). One subject had to be excluded from the analysis because he did not complete the study. Once they had performed a 5 min session of resting-state EEG recordings with their eyes closed, we assessed the perceived workload of 21 subjects when exposed to two different feedback tasks in a cross-over design and in pseudo-randomized order (see also figure 1): (i) BRI use with haptic/proprioceptive feedback of motor imagery-related sensorimotor oscillations, and (ii) control of neuromuscular activity with feedback of the EMG of the same hand. The tasks were separated by a 5 min break. Immediately after each task, the perceived workload was assessed with the NASA-TLX [34]. All subjects gave their written informed consent to participate in the study, which

was approved by the ethical review committee of the local medical faculty.

Electrophysiological recordings

In both tasks, EEG was recorded at a sampling rate of 1000 Hz at 31 channels (FP1, FP2, F3, Fz, F4, FC5, FC3, FC1, FCz, FC2, FC4, FC6, C5, C3, C1, Cz, C2, C4, C6, CP5, CP3, CP1, CPz, CP2, CP4, CP6, P3, Pz, P4, O1, O2), grounded to AFz, and referenced to TP10 on the right mastoid. Surface EMG was recorded at a sampling rate of 1000 Hz with adhesive EMG electrodes on the abductor pollicis brevis (APB), first dorsal interosseus (FDI), flexor digitorum superficialis (FDS) and extensor digitorum communis (EDC). Data was transmitted online to BCI2000 for classification [39] and stored for offline processing with Fieldtrip [35] and custom written scripts.

Resting-state EEG

Resting-state EEG was recorded for 5 min, with subjects instructed to sit with their eyes closed in a relaxed and comfortable position. After down-sampling to 500 Hz, we used a zero-phase lag FIR filter (first order) to filter the resting-state EEG collected for the estimation of sensorimotor power with a band-pass filter between 6 and 16 Hz. We divided the signal into epochs of 2 s length, automatically rejecting any epochs containing artifacts with an amplitude >200 μV. We calculated the phase slope index (Ψ and Ψ_{net}) for the frequency range from 8 to 14 Hz with a frequency resolution of 1 Hz [29], according to the following formula:

$$\Psi_{ij}(f) = \frac{\sum_{e=1}^{E} \mathrm{sgn}\left(\Im\left(\sum_{f\in F} C_{ij}^{*}(f,e)\,C_{ij}(\mathrm{f}+\delta f,e)\right)\right)}{E},$$

where C_{ij} denotes the complex coherency between channels i and j, δf represents the frequency resolution and $\Im()$ denotes the imaginary part. Since the sign of Ψ or Ψnet within each epoch indicates whether the channel is a sender (positive sign) or a receiver (negative sign), it can be averaged over epochs e, giving the likelihood that a connection between two channels i and j is sending or receiving information.

Accordingly, the likelihood that a channel i is a net transmitter or receiver was calculated as follows:

$$\psi_{\mathrm{net}}(i) = \frac{\sum_{e=1}^{E} \mathrm{sgn}\left(\sum_{j}\left(\Im\left(\sum_{f\in F} C_{ij}^{*}(f,e)\,C_{ij}(\mathrm{f}+\delta f,e)\right)\right)\right)}{E}.$$

Task-related EEG

The electrophysiological data was analyzed offline. EEG signals were down-sampled to 200 Hz, divided into non-overlapping epochs of 2s length and filtered below 48 Hz using a two-pass Butterworth low-pass filter with a filter order 4. Artifacts based on a range greater than 200 μV or a kurtosis larger than six were detected automatically. Artifacted channels were repaired using spherical spline interpolation. Epochs containing artifacts were rejected. We used multitaper frequency transformation to estimate the frequency power from 1 to 40 Hz, employing discrete prolate spheroidal sequences with a frequency smoothing of 2 Hz. The power spectrum was averaged across both task conditions to determine a task-independent power spectrum and normalized by z-scoring for each subject.

BRI task

In this task, the subjects' fingertips were attached to a hand robot (Amadeo, Tyromotion, Graz, Austria). This robot provided haptic/proprioceptive feedback contingent to motor imagery-related desynchronization of cortical oscillations recorded with EEG. Subjects controlled this BRI by volitional control of their sensorimotor oscillations in the beta-band as described in detail previously [27, 36, 37]. In each trial, subjects were instructed to prepare for motor imagery following a 'left hand' auditory cue (2 s preparation phase), and to imagine opening of the left hand following a 'start' cue (6 s motor imagery phase), which was followed by a 'rest' cue (6 s rest phase).

Every 40 ms, we estimated the power of three frequency bins (17,19 and 21 Hz) for the EEG contacts FC4, C4 and CP4, i.e. overall nine features, using an autoregressive model based on the Burg algorithm with a model order [38] of 16 and a sliding 500 ms window length, i.e. updated every 40 ms, to stay consistent with our earlier neurofeedback studies [27, 36, 37] thereby resulting in overlapping windows for the power estimation. The power of each channel and frequency bin was added with equal weight, resulting in a compound feature indicating the current sensorimotor power in the β-range. The mean and standard deviation of the rest condition were estimated on the basis of the last 375 × 40 ms measurements of this compound feature resulting in a 15 s period. During the motor imagery phase, the sensorimotor power in the β-range was estimated every 40 ms and normalized by the standard deviation of the rest condition. The resulting normalized power values were subsequently contrasted to the rest condition resulting in a sample to feature ratio of around 375 to 9. Due to the normalization and the predetermined feature weights, the classifier can be considered heavily regularized. This approach was chosen to ensure stability of the treatment rationale, i.e. reinforcing beta-band ERD in sensorimotor areas [10, 11, 13]. In this respect, the classification approach resembles a linear discrimination task by separating rest and motor imagery on the basis of thresholding event-related desynchronization [27, 36]. This approach was chosen due to the small number of features and their large covariance; when evaluating data with more features and unequal variance, shrinkage linear discriminant analysis might be considered. Whenever the beta-band desynchronization during the motor imagery phase reached the threshold ω, the robot opened the hand, or ceased its movement as soon as the threshold ω was not reached. In the rest phase, the robot returned the hand to the starting position. Subjects performed three runs, each of which consisted of 20 trials. Following each run, the threshold ω was

raised (from 0 to 0.9 to 1.4), which is equivalent to increasing the level of difficulty. The relative time in which the volitional modulation of oscillatory activity reached the threshold—indicating that the subject was able to control the robot—was averaged across difficulties and used as an indicator for task performance.

EMG feedback task

In this task, subjects volitionally controlled a certain muscle of their left hand and received feedback on the appropriate EMG activity. Current neuromuscular activity was calculated on the basis of the number of zero crossings within the last 500 ms [41]. Feedback was shown on a screen in front of the subjects in the form of a ball moving up and down. In each trial, subjects were requested to maintain their neuromuscular activity at a certain target level. The target level was indicated by a rectangular box at a certain height, and target levels were randomized between trials. In addition, the color of the ball turned from red to green as soon as the target level was reached. We increased the difficulty of the task by providing feedback for one, two or four muscles at a time, i.e. 24 trials with single muscle feedback (APB, FDI, FDS and EDC), 18 trials with two muscle feedback (APB & FDI, APB & FDS and FDS & EDC) and 18 trials with four muscle feedback. The feedback phase for the single muscle feedback lasted 10 s and was followed by a 5 s rest phase, while the feedback phase for the multiple muscles lasted 15 s. The relative time in which the modulation of neuromuscular activity lay within target range during the feedback phase—indicating that the subject was able to control neuromuscular activity—was averaged across difficulties and used as an indicator for task performance.

NASA Task Load Index (NASA-TLX)

Following each task, the subjects were asked to rate the relative importance of six task aspects on the basis of the NASA-TLX [34]: mental demand, physical demand, temporal demand, performance, frustration and efficacy. These six components of the NASA-TLX were presented in pairs and subjects were requested to choose which component in each pair they felt had exerted a higher impact on the task. All 15 possible combinations of components were presented in random order on a screen. Each component was represented by text and a specific icon for better recognition. The subjects received explanatory information about all components, e.g. how much feedback on their performance was important, whether they had to cope with frustration during the task or if they had the impression that their efforts had paid off in the task. After all pair-wise comparisons had been carried out each component received a relative ranking. The ratings for each task were averaged across subjects as an indicator of the task-specific workload.

Statistical analysis

Based on the Calinski–Harabasz criterion, two clusters were considered optimal within the search space of up to five clusters. We used the *K*-means clustering algorithm as implemented in Matlab (100 repetitions, squared Euclidean distance) to group subjects into two clusters for each task on the basis of their workload profile. We performed a visual inspection of the scatter plots to assess the resulting cluster validity. Additionally, we contrasted the results of the cluster analysis with a simulation based on clustering 1000 iterations of white noise with a dimensionality identical to our dataset (i.e. $m=6$, $n=21$), to assess the probability of false positive clustering. Distribution of the cross-tabulated cluster membership was tested with Fisher's exact test. Normality was assessed using the Kolmogorov–Smirnov test. Normality was established for the difference in NASA-TLX values between the tasks and within the clusters. We used a *t*-test to detect any significant differences between clusters and tasks. If normality was not established, we used Spearman's rank correlation; otherwise we calculated Pearson's correlation coefficient. Where applicable, Bonferonni correction was used to account for multiple comparisons. Differences in the power spectrum and network activity of the clusters were tested with a Kruskal–Wallis test. In all statistical tests, an alpha error of $p<0.05$ was assumed to be significant.

Results

Workload profile

The BRI and the EMG tasks were of a similar difficulty for the subjects, i.e. the respective task performances did not differ ($t(20)=1.89$, $p>0.07$). However, since the tasks addressed different demands, there was no correlation between the performance in each of the tasks ($r=0.08$, $p>0.74$). The physical demand ($t(20)=3.25$, $\Delta=1.34$, $p=0.004$) was rated as being more important in the EMG task, whereas frustration ($t(20)=3.54$, $\Delta=0.86$, $p=0.002$) was deemed more important in the BRI task (figure 2). However, perceived frustration was correlated across tasks (Pearson's $r=0.72$, $p=0.0002$), indicating a task-independent, i.e. subject-specific relevance of this workload component.

Clustering of workload profiles

The clustering of the BRI-profile revealed two groups (BRI_1 and BRI_2) which, although similar with regard to their task-performance ($t(19)=0.59$, $p>0.55$), could be distinguished by their levels of frustration and efficacy (see figure 3(A)): The first group (BRI_1, $n=12$) experienced lower frustration ($t(19)=3.82$, $\Delta=-1.56$, $p=0.001$) and higher efficacy ($t(19)=6.36$, $\Delta=2.72$, $p<0.001$) than the second (BRI_2, $n=9$). The clustering of the EMG-profile revealed two groups (EMG_1 and EMG_2) which were similar with regard to their task-performance ($t(19)=0.85$, $p>0.40$), but which could be distinguished by their physical, mental and temporal demands (see figure 3(B)). The first group (EMG_1, $n=12$) experienced lower physical demands ($t(19)=10.96$, $\Delta=-2.92$, $p<0.001$), but higher mental ($t(19)=4.63$, $\Delta=2.53$, $p=0.002$) and

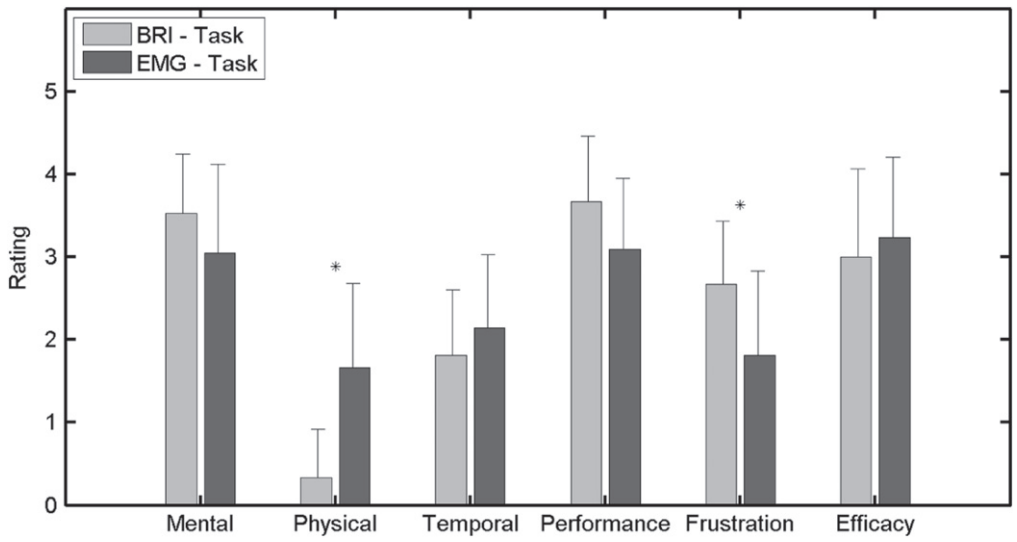

Figure 2. Comparison of workload profiles. The average workload profiles for the BRI and EMG task are depicted here. Asterisks indicate significant differences at the $p < 0.05$ level and error bars indicate 95% confidence intervals (with Bonferroni correction).

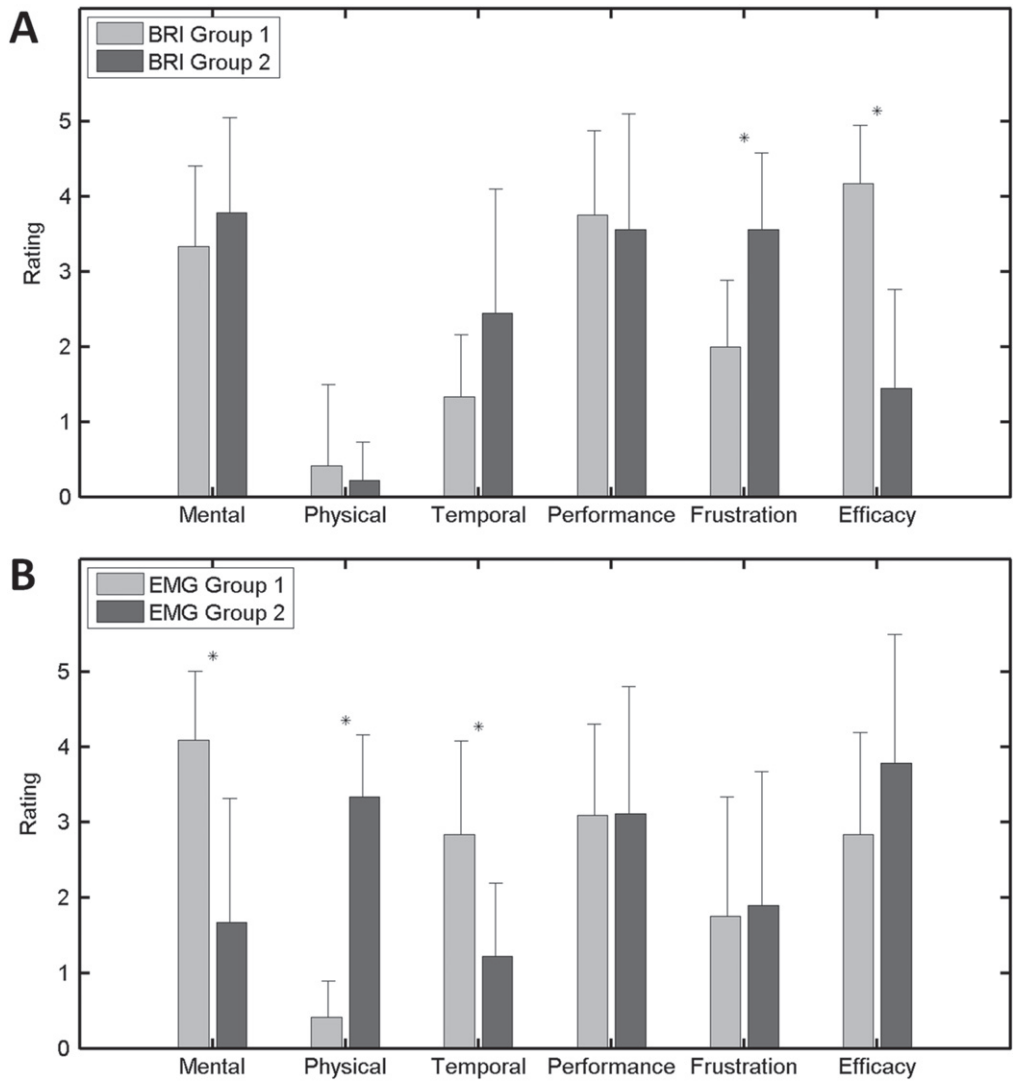

Figure 3. Workload profiles of the clustered BRI (A) and EMG (B) groups. The ratings indicate the average perceived workload of each group for each of the six NASA-TLX dimensions (*x*-axis). Asterisks indicate significant differences at $p < 0.05$ level and error bars indicate 95% confidence intervals (both with Bonferroni correction).

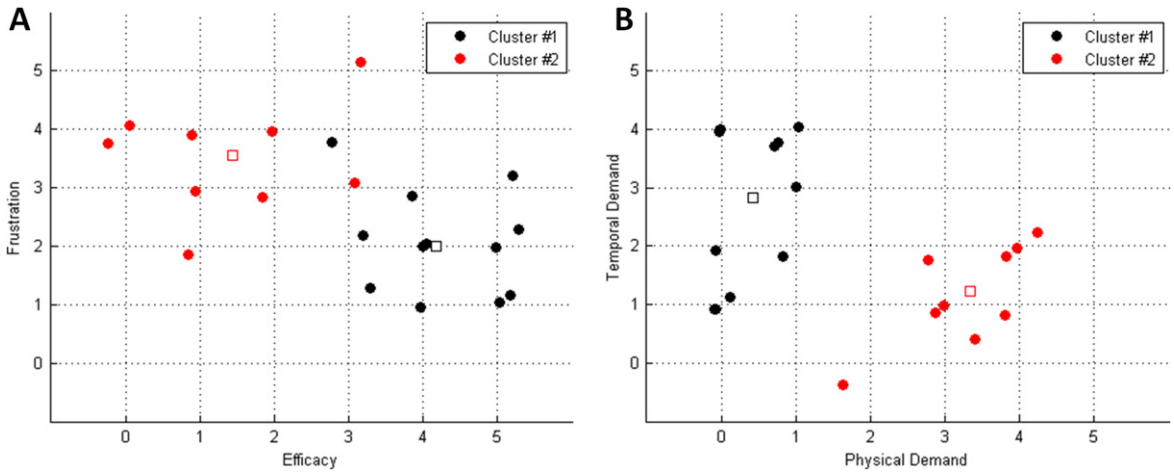

Figure 4. Shows the cluster validity for the dimensions with significant differences between the clusters. (A) Shows the differences for BRI-TLX for the dimensions frustration and efficacy; (B) shows the differences for EMG-TLX for the dimensions temporal and physical demands. Black dots indicate membership to cluster 1, red dots membership to cluster 2. Squares indicate cluster centroids. Please note that jitter was added to prevent points from overlying each other.

Table 1. Cross-table of group membership showing the group size for the groups based on within-task differences of the workload profiles.

		BRI feedback	
		Low frustration 'BRI_1'	High frustration 'BRI_2'
EMG feedback	Low physical demand 'EMG_1'	$N=8$	$N=4$
	High physical demand 'EMG_2'	$N=4$	$N=5$

temporal demands ($t(19)=3.17$, $\Delta=1.61$, $p=0.005$) than the second (EMG_2, $n=9$).

Visual inspection of the scatter plots indicated appropriate clustering (see figure 4 for representative scatter plots for each task). Additionally, simulation with white noise indicated the probability of false positive clustering to be 13.6% and 4.3% for the BRI-task and EMG-task, respectively.

Eight subjects were part of both BRI_1 and EMG_1, constituting a group (BRI_1/EMG_1) with low frustration during the BRI task and low physical demand during EMG-task. Five subjects were part of both BRI_2 and EMG_2, constituting a group (BRI_2/EMG_2) with high frustration during the BRI task and high physical demand during EMG-task (see table 1). The fact that we did not find a significant difference in the distribution (Fisher's exact test, $p>0.21$), is indicative of independence of group membership.

Neurophysiological comparison

On comparing the two groups of each task, i.e. BRI_1 versus BRI_2 and EMG_1 versus EMG_2, respectively, we detected significant differences with regard to their electrophysiological activity during resting-state and during the task.

In the resting-state, subjects in the BRI_1 group (see figure 5(A)) and in the EMG_1 group (see figure 5(B)) exhibited a stronger sending from left parietal regions to right frontal and central areas than subjects in the BRI_2 group and the EMG_2 group, respectively. The difference pattern established for the EMG task was highly correlated with that of the BRI task (for $L\Psi_{net}$: Pearson's $r=0.68$, $p<0.001$, for $L\Psi$: Pearson's $r=0.34$, $p<0.001$). In addition, a comparison between the diagonal groups, i.e. the 'BRI_1/EMG_1' and the 'BRI_2/EMG_2' group, showed that this pattern was strongly expressed as well (see figure 5(C)).

During the task, these groups also showed striking differences in their averaged electrophysiological activity. Power was increased particularly in the theta-range (see figure 6(A)). The topographical analysis revealed that subjects in the BRI_1 group (see figure 6(B)) and in the EMG_1 group (see figure 6(C)), but not in the BRI_2 group and the EMG_2 group, exhibited increased theta power, with a sensorimotor hotspot contralateral to the moved hand. Furthermore, this topographical pattern was highly correlated between the tasks (Pearson's $r=0.73$, $p<0.001$), and strongly expressed in a comparison between the diagonal groups, i.e. 'BRI_1/EMG_1' and 'BRI_2/EMG_2' (see figure 6(D)).

Discussion

When examining the workload profile of two neurorehabilitation tasks, BRI feedback differed from EMG feedback, particularly with regard to the experience of frustration. Moreover, the frustration level was highly correlated across tasks, indicating that this component of the workload profile was linked to subject characteristics. Those subjects who were specifically challenged by the respective tasks could be detected by an interhemispheric alpha-band network in

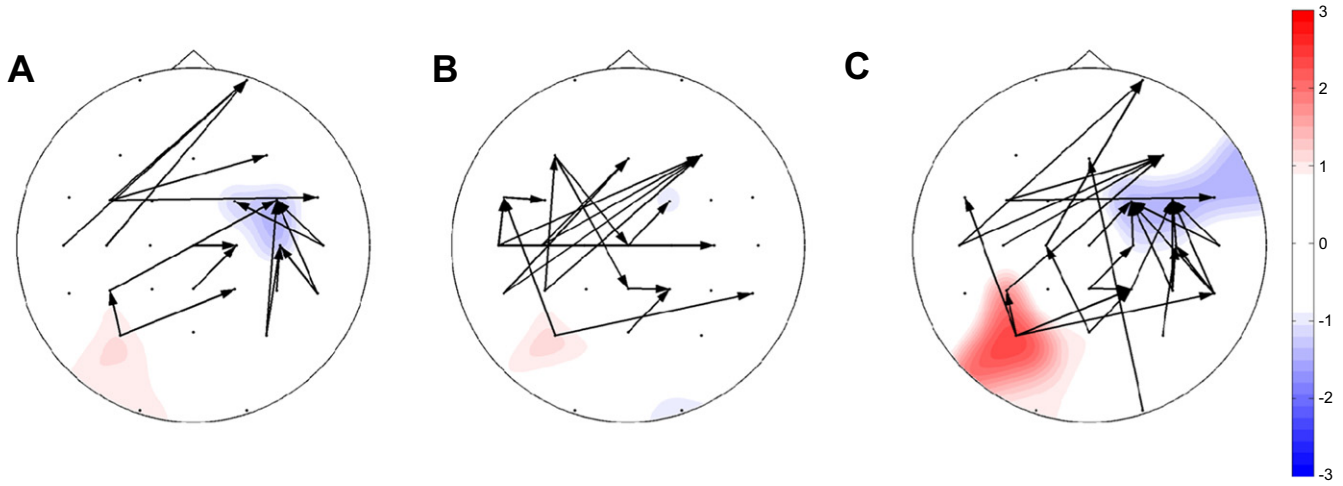

Figure 5. Resting state neurophysiological differences due to cluster membership. The figure shows the topography of differences in alpha-range (8–14 Hz) of network activity during resting state. For $L\Psi_{net}$, saturation of the colors indicates significance level on a log10 scale. Red colors indicate positive and blue colors negative mean difference. Since $L\Psi$ is asymmetric, only positive significant values are depicted with arrows pointing in the direction of sending. (A) Activation pattern of the BRI_1 group compared to the BRI_2 group. (B) Activation pattern of the EMG_1 group compared to the EMG_2 group. (C) Activation pattern of the BRI_1/EMG_1 group compared to the BRI_2/EMG_2 group.

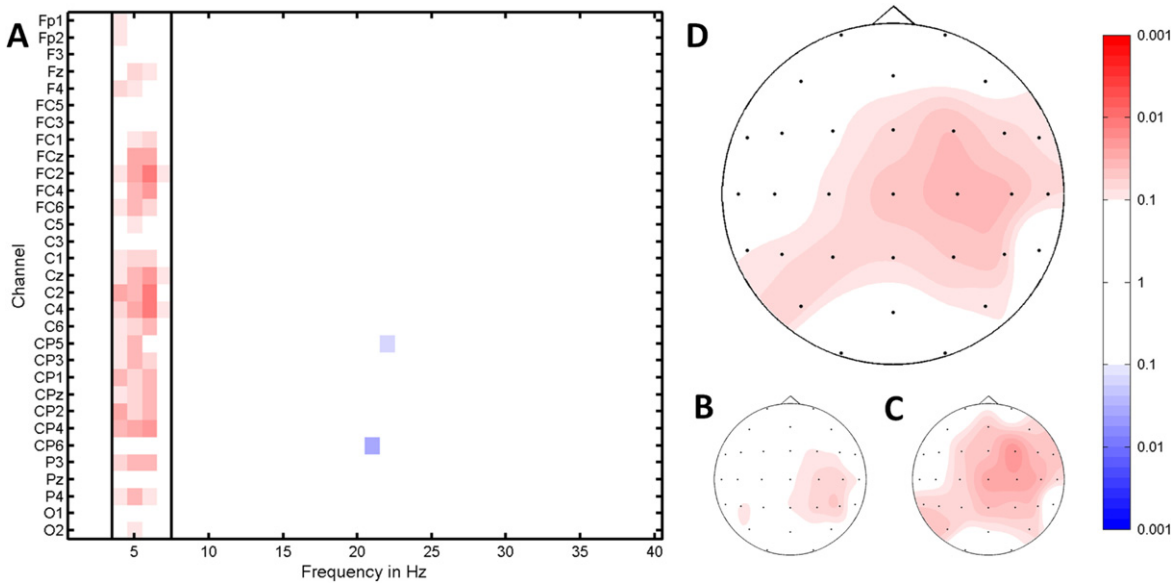

Figure 6. Task-based neurophysiological differences due to cluster membership. (A) Heat map of significance levels showing differences in average task-related power between the BRI_1/EMG_1 group and the BRI_2/EMG_2 group on a directed log10 scale with frequency (in Hz) on the *x*-axis and channels on the *y*-axis. Blue colors indicate decreased, red colors increased power for the BRI_1/EMG_1 group. Please note the increased power in the theta range (4–7 Hz). (B)–(D) Show topography of power differences averaged across the theta range (4–7 Hz). (B) Activation pattern of the BRI_1 group compared to the BRI_2 group (C) activation pattern of the EMG_1 group compared to the EMG_2 group (D) activation pattern of the BRI_1/EMG_1 group compared to the BRI_2/EMG_2 group.

resting state *before* the training and by their sensorimotor theta-band activation pattern *during* the exercise.

Workload profile

Despite the fact that the participants in our study were healthy young adults, some of them were significantly challenged when confronted with the task of using a brain-controlled robotic device designed for restorative purposes, namely for the modification of neuronal activity via operant conditioning. They experienced frustration when dealing with this novel approach, even though the robot was attached to their hand and provided haptic/proprioceptive feedback of the volitional modulation of brain activity; an approach which facilitates the detection of motor intention [42] and the self-regulation of sensorimotor beta-band activity [37]. These findings therefore indicate that further optimization of BRI training may be required to address the cognitive resources of participants [42]. This concept is endorsed by the observation that the frustration level was highly correlated across tasks, indicating

that this component of the workload profile was task-independent, and thus supporting the notion that the perceived workload was influenced by the characteristics of the individual subject.

Neurophysiological profiles

In resting state, the less challenged groups, i.e. BRI_1, EMG_1 and BRI_1/EMG_1, showed a network pattern in the alpha band that sent from left parietal regions to right frontal and central areas (see figure 5). Remarkably, the very same groups also showed a highly correlated pattern during the task, exhibiting increased theta power in the right sensorimotor area, i.e. contralateral to the moved hand, and in the left parietal region (see figure 6). These observed patterns of cortical neurophysiology tally well with those reported previously [27, 36, 37]. More specifically, resting state alpha-band networks between left parietal and right frontal and central areas predict the *ability* for motor imagination and motor execution across a battery of motor tasks, including EMG- and BRI-feedback [27]. The present study shows that these resting state alpha-band networks also predict the *perceived task challenge*. During the task, functional coupling in the theta-band contralateral to the trained hand correlates with the *skill* of brain-self regulation during BRI [37]. Theta power has been proposed as an indicator of cognitive demands [43] and has also been implicated in sensorimotor integration and motor learning [44, 45]. The present study extends this line of research by the observation that differences in theta power contralateral to the trained hand are also connected to the *perceived task challenge*.

Although these neurophysiological findings require further validation, they might already provide building blocks for the development of reliable and general biomarkers for workload assessment in the context of neurofeedback training. Patterns of cortical alpha-network activity, acquired in short screening sessions before the training, might, for example, predict the probability of being challenged by the following exercise and theta-band activity during the task exercise might provide information about current cognitive resources available to the participants.

Matching subjects' ability and task difficulty

Since the level of frustration was highly correlated across tasks and neurophysiological correlates indicated a relationship to cognitive load and early motor learning, this knowledge might be used to match the task difficulty and the participants' ability for learning [12], known as the zone of proximal development [17]. This might be particularly important for neurological patients with cognitive impairments, e.g. following stroke, where a substantial number of—sometimes even young—patients must cope with long-term or even permanent cognitive deficits [20]. In addition, further possible strategies might not only focus on matching subjects' ability and task difficulty, but also on the goal of decreasing the cognitive load by cueing during the task [46] or by implementing breaks and increasing inter-trial-intervals [47, 48].

One practical approach could therefore use the breaks between runs to assess the subjects' level of frustration. A simple self-rating question, such as 'Was this setting too difficult or too simple for you?' would be a straightforward and fast way of adjusting the task difficulty to individual resources [49]. Moreover, the neurophysiological markers could provide the target substrate for adjunct interventions, such as online-adaptation of the difficulty, initiating breaks or inducing exogenous theta synchronization by using transcranial alternating current stimulation to improve task performance [50, 51].

Conclusions

Brain–robotic interface feedback exhibited a distinct workload profile which differed from electromyographic neurofeedback. However, high levels of task-specific challenge in each of these interventions were linked to the same neurophysiological correlates. Resting state alpha-band networks and task-related theta-band activity characterized those subjects who were particularly challenged in each of these feedback tasks. Therefore, these neurophysiological profiles represented task-independent markers of workload and may serve as biomarkers for monitoring and matching participant's ability and task difficulty.

Acknowledgments

RB was supported by the Graduate Training Centre of Neuroscience, International Max Planck Research School for Cognitive and Systems Neuroscience, Tuebingen, Germany. AG was supported by grants from the German Research Council [DFG GH 94/2-1, DFG EC 307], and from the Federal Ministry for Education and Research [BFNT 01GQ0761, BMBF 16SV3783, BMBF 03160064B, BMBF V4UKF014]. There is no conflict of interest.

References

[1] Kwakkel G, Kollen B J, van der Grond J and Prevo A J H 2003 Probability of regaining dexterity in the flaccid upper limb: impact of severity of paresis and time since onset in acute stroke *Stroke* **34** 2181–6

[2] Pollock A, Farmer S E, Brady M C, Langhorne P, Mead G E, Mehrholz J and van Wijck F 2014 Interventions for improving upper limb function after stroke *Cochrane Database Syst. Rev.* **11** CD010820

[3] Langhorne P, Coupar F and Pollock A 2009 Motor recovery after stroke: a systematic review *Lancet Neurology* **8** 741–54

[4] Armagan O, Tascioglu F and Oner C 2003 Electromyographic biofeedback in the treatment of the hemiplegic hand: a placebo-controlled study *Am. J. Phys. Med. Rehabil.* **82** 856–61

[5] Woodford H and Price C 2007 EMG biofeedback for the recovery of motor function after stroke *Cochrane Database Syst. Rev.* **18** CD004585
[6] Doğan-Aslan M, Nakipoğlu-Yüzer G F, Doğan A, Karabay I and Özgirgin N 2012 The effect of electromyographic biofeedback treatment in improving upper extremity functioning of patients with hemiplegic stroke *J. Stroke Cerebrovasc. Dis.* **21** 187–92
[7] Ramos-Murguialday A *et al* 2013 Brain–machine-interface in chronic stroke rehabilitation: a controlled study *Ann. Neurology* **74** 100–8
[8] Ang K K, Guan C, Phua K S, Wang C, Zhou L, Tang K Y, Ephraim J G J, Kuah C W K and Chua K S G 2014 Brain–computer interface-based robotic end effector system for wrist and hand rehabilitation: results of a three-armed randomized controlled trial for chronic stroke *Front. Neuroeng.* **7** 30
[9] Cincotti F, Pichiorri F, Aricò P, Aloise F, Leotta F, de Vico F F, Millán J del R, Molinari M and Mattia D 2012 EEG-based brain–computer interface to support post-stroke motor rehabilitation of the upper limb *Proc. IEEE Conf. of the Engineering in Medicine and Biology Society (EMBC)* pp 4112–5
[10] Rossiter H E, Boudrias M-H and Ward N S 2014 Do movement-related beta oscillations change following stroke? *J. Neurophysiol.* **112** 2053–8
[11] Takemi M, Masakado Y, Liu M and Ushiba J 2013 Event-related desynchronization reflects downregulation of intracortical inhibition in human primary motor cortex *J. Neurophysiol.* **110** 1158–66
[12] Bauer R and Gharabaghi A 2015 Estimating cognitive load during self-regulation of brain activity and neurofeedback with therapeutic brain–computer interfaces *Front. Behav. Neurosci.* **9**
[13] Bauer R and Gharabaghi A 2015 Reinforcement learning for adaptive threshold control of restorative brain–computer interfaces: a Bayesian simulation *Front. Neurosci.* **9**
[14] Kaiser V, Kreilinger A, Müller-Putz G R and Neuper C 2011 First steps toward a motor imagery based stroke BCI: new strategy to set up a classifier *Front. Neurosci.* **5**
[15] Faller J, Scherer R, Friedrich E V C, Costa U, Opisso E, Medina J and Müller-Putz G R 2014 Non-motor tasks improve adaptive brain–computer interface performance in users with severe motor impairment *Front. Neurosci.* **8** 320
[16] Kirschner P A 2002 Cognitive load theory: implications of cognitive load theory on the design of learning *Learn. Instr.* **12** 1–10
[17] Schnotz W and Kürschner C 2007 A reconsideration of cognitive load theory *Educ. Psychol. Rev.* **19** 469–508
[18] Hammer E M, Halder S, Blankertz B, Sannelli C, Dickhaus T, Kleih S, Müller K-R and Kübler A 2012 Psychological predictors of SMR-BCI performance *Biol. Psychol.* **89** 80–6
[19] De Vries S, Tepper M, Otten B and Mulder T 2011 Recovery of motor imagery ability in stroke patients *Rehabil. Res. Pract.* **2011** 283840
[20] Schaapsmeerders P, Maaijwee N A M, van Dijk E J, Rutten-Jacobs L C A, Arntz R M, Schoonderwaldt H C, Dorresteijn L D A, Kessels R P C and de Leeuw F-E 2013 Long-term cognitive impairment after first-ever ischemic stroke in young adults *Stroke* **44** 1621–8
[21] Thomas E, Dyson M and Clerc M 2013 An analysis of performance evaluation for motor-imagery based BCI *J. Neural Eng.* **10** 031001
[22] Thompson D E *et al* 2014 Performance measurement for brain–computer or brain–machine interfaces: a tutorial *J. Neural Eng.* **11** 035001
[23] Riccio A, Leotta F, Bianchi L, Aloise F, Zickler C, Hoogerwerf E-J, Kübler A, Mattia D and Cincotti F 2011 Workload measurement in a communication application operated through a P300-based brain–computer interface *J. Neural Eng.* **8** 025028
[24] NASA Human Performance Research Group 1986 *TLX Paper and Pencil Version Instruction Manual* (Moffet Field, CA: NASA Ames Research Center)
[25] Cegarra J and Chevalier A 2008 The use of Tholos software for combining measures of mental workload: toward theoretical and methodological improvements *Behav. Res. Methods* **40** 988–1000
[26] Vidaurre C and Blankertz B 2010 Towards a cure for BCI illiteracy *Brain Topogr.* **23** 194–8
[27] Bauer R, Fels M, Vukelić M, Ziemann U and Gharabaghi A 2014 Bridging the gap between motor imagery and motor execution with a brain–robot interface *NeuroImage* **108** 319–27
[28] Nolte G, Ziehe A, Krämer N, Popescu F and Müller K-R 2010 Comparison of granger causality and phase slope index *J. Mach. Learn. Res. W&CP* **6** 267–76
[29] Nolte G, Ziehe A, Nikulin V V, Schlögl A, Krämer N, Brismar T and Müller K-R 2008 Robustly estimating the flow direction of information in complex physical systems *Phys. Rev. Lett.* **100** 234101
[30] Haufe S, Nikulin V V, Müller K-R and Nolte G 2013 A critical assessment of connectivity measures for EEG data: a simulation study *Neuroimage* **64** 120–33
[31] Smith M E, Gevins A, Brown H, Karnik A and Du R 2001 Monitoring task loading with multivariate EEG measures during complex forms of human–computer interaction *Hum. Factors: J. Hum. Factors Ergon. Soc.* **43** 366–80
[32] Demanuele C, Broyd S J, Sonuga-Barke E J S and James C 2012 Neuronal oscillations in the EEG under varying cognitive load: a comparative study between slow waves and faster oscillations *Clin. Neurophysiol.* **124** 247–62
[33] Novak D, Mihelj M and Munih M 2010 Psychophysiological responses to different levels of cognitive and physical workload in haptic interaction *Robotica* **29** 367–74
[34] Hart S 2006 Nasa-task load index (Nasa-TLX); 20 years later *Proc. Human Factors and Ergonomics Society Annual Meeting* pp 904–8
[35] Oostenveld R, Fries P, Maris E and Schoffelen J-M 2011 FieldTrip: open source software for advanced analysis of MEG, EEG, and invasive electrophysiological data *Comput. Intell. Neurosci.* **2011** 1–9
[36] Vukelić M, Bauer R, Naros G, Naros I, Braun C and Gharabaghi A 2014 Lateralized alpha-band cortical networks regulate volitional modulation of beta-band sensorimotor oscillations *NeuroImage* **87** 147–53
[37] Vukelić M and Gharabaghi A 2015 Oscillatory entrainment of the motor cortical network during motor imagery is modulated by the feedback modality *Neuroimage* **111**
[38] McFarland D J and Wolpaw J R 2008 Sensorimotor rhythm-based brain-computer interface (BCI): model order selection for autoregressive spectral analysis *J. Neural Eng.* **5** 155–62
[39] Schalk G, McFarland D J, Hinterberger T, Birbaumer N and Wolpaw J R 2004 BCI2000: a general-purpose brain–computer interface (BCI) System *IEEE Trans. Biomed. Eng.* **51** 1034–43
[40] Gharabaghi A, Kraus D, Leão M T, Spüler M, Walter A, Bogdan M, Rosenstiel W, Naros G and Ziemann U 2014 Coupling brain–machine interfaces with cortical stimulation for brain-state dependent stimulation: enhancing motor cortex excitability for neurorehabilitation *Front. Hum. Neurosci.* **8** 122
[41] Inbar G F, Allin J, Paiss O and Kranz H 1986 Monitoring surface EMG spectral changes by the zero crossing rate *Med. Biol. Eng. Comput.* **24** 10–8
[42] Jann K, Koenig T, Dierks T, Boesch C and Federspiel A 2010 Association of individual resting state EEG alpha frequency and cerebral blood flow *Neuroimage* **51** 365–72

[43] Lundqvist M, Herman P and Lansner A 2011 Theta and gamma power increases and alpha/beta power decreases with memory load in an attractor network model *J. Cogn. Neurosci.* **23** 3008–20

[44] Caplan J B, Madsen J R, Schulze-Bonhage A, Aschenbrenner-Scheibe R, Newman E L and Kahana M J 2003 Human theta oscillations related to sensorimotor integration and spatial learning *J. Neurosci.* **23** 4726–36

[45] Cruikshank L C, Singhal A, Hueppelsheuser M and Caplan J B 2011 Theta oscillations reflect a putative neural mechanism for human sensorimotor integration *J. Neurophysiol.* **107** 65–77

[46] Heremans E, Nieuwboer A, Feys P, Vercruysse S, Vandenberghe W, Sharma N and Helsen W F 2012 External cueing improves motor imagery quality in patients with Parkinson disease *Neurorehabil. Neural Repair* **26** 27–35

[47] Albert N B, Robertson E M, Mehta P and Miall R C 2009 Resting state networks and memory consolidation *Commun. Integr. Biol.* **2** 530–2

[48] Dewar M, Alber J, Butler C, Cowan N and Della S S 2012 Brief wakeful resting boosts new memories over the long term *Psychol. Sci.* **23** 955–60

[49] Clark R C 2006 *Efficiency in Learning: Evidence-Based Guidelines to Manage Cognitive Load* (San Francisco: Jossey-Bass)

[50] Feurra M, Pasqualetti P, Bianco G, Santarnecchi E, Rossi A and Rossi S 2013 State-dependent effects of transcranial oscillatory currents on the motor system: what you think matters *J. Neurosci.* **33** 17483–9

[51] Polanía R, Nitsche M A, Korman C, Batsikadze G and Paulus W 2012 The importance of timing in segregated theta phase-coupling for cognitive performance *Curr. Biol.* **22** 1314–8